Applied Catalysis B: Environmental 225 (2018) 406–414

Contents lists available at ScienceDirect

Applied Catalysis B: Environmental

journal homepage: www.elsevier.com/locate/apcatb

Visible light-induced catalytic activation of peroxymonosulfate using heterogeneous surface complexes of amino acids on TiO_2

Jonghun Lim[a,1], Dong-yeob Kwak[a,1], Fabian Sieland[b], Chuhyung Kim[a], Detlef W. Bahnemann[b], Wonyong Choi[a,*]

[a] Division of Environmental Science and Engineering and Department of Chemical Engineering, Pohang University of Science and Technology (POSTECH), Pohang 37673, Republic of Korea

[b] Leibniz University Hannover, Institute of Technical Chemistry, 30167 Hannover, Germany; Laboratory "Photoactive Nanocomposite Materials", Saint-Petersburg State University, Saint-Petersburg, 198504, Russia

ARTICLE INFO

Keywords:
Visible light activation of PMS
Sulfate radical
Amino acid degradation
Surface complex
Advanced oxidation process (AOP)

ABSTRACT

Peroxymonosulfate (PMS) is being extensively investigated as an eco-friendly oxidant and various activation methods of PMS have been investigated. Here we demonstrated a new method of catalytic PMS activation, which employed amino acids as both a visible light sensitizer and a substrate to be degraded. Although PMS and amino acids do not absorb any visible light, the surface adsorption of amino acids on titania formed charge-transfer complexes that absorb visible light ($\lambda > 420$ nm). Serine and histidine were employed as main target amino acids and their surface complexes on TiO_2 were characterized by various spectroscopic methods The ligand-to-metal charge transfer between amino acids and TiO_2 enabled the absorption of visible light and the subsequent electron transfer catalytically activated PMS with generating sulfate radicals which were detected by electron paramagnetic resonance analysis. Based on various scavenger tests, amino acids seem to be degraded mainly by sulfate radical (radical pathway) and by a non-radical pathway (PMS serving primarily as an electron acceptor) to some extent. Amino acids were degraded with producing ammonium as a sole nitrogenous product in this process, whereas most advanced oxidation processes of amino acid generate not only ammonium but also nitrate and nitrite. The visible light-induced charge transfer characteristics of the amino acid-TiO_2 complexes were demonstrated by the photoelectrochemical characterizations and the time-resolved laser spectroscopic analysis.

1. Introduction

Amino acids are main components of biological organisms and a huge amount of amino acids (3.3 millions of tons) are released to natural waters from pharmaceutical, cosmetic, and food industries [1]. The release of amino acids is detrimental to the environment because their oxidation leads to the generation of hazardous nitrogen compounds such as nitrate and nitrite and the introduction of nitrogen compounds to aquatic environment accelerates the algal growth causing eutrophication [2–4]. One of the most popular methods to decompose amino acids in wastewater streams is the chlorination treatment [5,6]. However, this method induces the formation of odorous disinfection byproducts (DBPs) such as trihalomethanes (THMs), haloacetic acids (HAAs), chloroamines (NH_2Cl), and cyanogen chloride (CNCl). Advanced oxidation processes (AOPs) such as TiO_2/UV have also been investigated for the degradation of amino acids because it is an environmentally benign technique utilizing sunlight only without the need of chemical oxidants [7]. However, the solar efficiency is limited by the lack of visible light absorption and the method generates not only ammonium but also harmful nitrate and nitrite as products from the decomposition of amino acids [1,8].

Activation of peroxymonosulfate (PMS) has been widely investigated for the degradation of aqueous pollutants through non-radical and radical pathways [9,10]. For a non-radical pathway, the direct electron transfer from organic pollutants to PMS through charge transfer catalysts induces the oxidation of organic pollutants with generating sulfate ions ($E^0(HSO_5^-/SO_4^{2-}) = 1.75\ V_{NHE}$) [11]. On the other hand, a radical pathway involves the generation of reactive sulfate radical ($E^0(HSO_5^-/SO_4^{\cdot -}) = 2.5–3.1\ V_{NHE}$) through PMS activation by catalysts or external energy input to cleave the peroxide bond [12]. The radical pathway has been more investigated than the non-radical pathway because sulfate radicals have strong oxidizing power in water over a wide pH range [13]. Various materials such as metal oxides [14,15], transition metals [16,17], and carbon materials [18–20]

* Corresponding author.
E-mail address: wchoi@postech.edu (W. Choi).
[1] These authors contributed equally to this work.

https://doi.org/10.1016/j.apcatb.2017.12.025
Received 26 October 2017; Received in revised form 5 December 2017; Accepted 10 December 2017
Available online 11 December 2017
0926-3373/

have been widely investigated for the activation of PMS. Photochemical activation of PMS has been also investigated using UV light [10,21,22] but a milder photochemical activation using visible light only is much desirable. Some visible light photocatalysts such as $ZnFe_2O_4$ [23] and $BiVO_4$ [24] have been employed for PMS activation but such materials are not appropriate as practical water treatment catalysts. The visible light activation of PMS on TiO_2 would be much favored considering that the practical merits of TiO_2 such as high abundance and availability, low cost, excellent stability, and non-toxicity [25,26]. Although TiO_2 has no photoactivity under visible light, the ligand-to-metal charge transfer (LMCT) induced by surface adsorbates is a possible mechanism that enables visible light absorption [25–27]. The surface complexation can induce the visible light absorption through direct charge transfer (CT) from the HOMO level of the adsorbate to the conduction band (CB) of TiO_2 [28,29]. Various adsorbates have been reported for the LMCT complexation with TiO_2 [30–33] and many other organic compounds are also potential candidates as a LMCT-sensitizer.

In this work, we investigated a new visible light-induced catalytic activation method of PMS by employing amino acids that serve as both a LMCT-sensitizer and a substrate to be degraded. Amino acids complexed with TiO_2 surface enable the absorption of visible light through LMCT mechanism and the generation of $SO_4\cdot^-$ from PMS. The catalytic oxidative mechanism of amino acids degradation under visible light was investigated by using various spectroscopic and photoelectrochemical methods and discussed in detail.

2. Materials and methods

2.1. Chemicals and materials

Chemical reagents used in this study are as follows: potassium peroxymonosulfate ($2KHSO_5\cdot KHSO_4\cdot K_2SO_4$ available as OXONE, PMS, Aldrich), L-Alanine (Ala, SAMCHUN), L-Glycine (Gly, Sigma-Aldrich), L-Histidine (His, Sigma-Aldrich), L-Phenylalanine (Phe, Alpha), L-Serine (Ser, SAMCHUN), methanol (J.T. Baker), *tert*-butanol (t-BuOH, Aldrich), hexavalent chromium (Cr(VI), $Na_2Cr_2O_7\cdot H_2O$, Aldrich), and 5,5-dimethyl-1-pyrroline-N-oxide (DMPO, Sigma-Aldrich), N,N-diethyl-1,4-phenylene-diamine sulfate (DPD, Sigma-Aldrich). All chemical reagents were used as received without any purification. Commercial TiO_2 powder (P25) with an average surface area of 50(± 15) $m^2\,g^{-1}$ and primary particle size of 20–30 nm was used as heterogeneous support. Ultrapure (14 MΩ cm) deionized water was used and prepared by a Barnstead purification system.

2.2. Characterization of amino acid complexed-TiO2

Serine and histidine complexed-TiO_2 (Ser- and His-TiO_2, respectively) powder for the sample characterization was prepared as follows. Amino acid (10 mM) was added to aqueous TiO_2 suspension and the pH was adjusted at pH 3 or 7. Then, the suspension was filtered and dried in an oven at 80 °C to recover powder. The ATR-FTIR spectra of the prepared samples were measured using a Thermo iS50 FT-IR spectrometer. The powder sample was put onto a ZnSe crystal and the spectra were collected. Diffuse reflectance UV/visible absorption spectra (DRS) were obtained by using a spectrophotometer (Shimadzu UV-2600) with an integrating sphere attachment and $BaSO_4$ was used as the reference. High resolution transmission electron microscopy (HR-TEM) and electron energy-loss spectroscopy were carried out on JEOL JEM-2200 FS (at NCNT) with the Cs-corrected line.

2.3. Photochemical reaction procedure and analysis

TiO_2 powder (1 g/L) was dispersed in distilled water by simultaneous sonication and shaking for 30 s in an ultrasonic cleaning bath. An aliquot of the substrate stock solution of amino acid and PMS solution was subsequently added to the suspension and then the initial pH of the suspension was adjusted with a standard solution of $HClO_4$ or NaOH. The aqueous suspension was stirred for 30 min for the equilibrium adsorption of amino acid and PMS on TiO_2. Photo-irradiation experiments employed a 300 W Xe arc lamp (Oriel). Light passed through a 10 cm IR water filter and a cut-off filter ($\lambda > 300$ nm for UV light and $\lambda > 420$ nm for visible light irradiation), and the filtered light was focused onto a 50-mL Pyrex reactor. The reactor was stirred magnetically during the reaction. Sample aliquots were intermittently withdrawn from the reactor during light irradiation and filtered through a 0.45 μm PTFE syringe filter (Millipore) for analysis.

The analyses of NH_4^+, NO_3^-, and NO_2^- generated from the degradation of amino acids were performed using an ion chromatograph (IC, Dionex DX-120) which was equipped with a Dionix IonPac AS 14 (4 mm × 250 mm) for anions, a Dionex IonPac CS 12A (4 mm × 250 mm) for cations, and a conductivity detector. The eluent solution was Na_2CO_3 (3.5 mM)/$NaHCO_3$ (1 mM) for anions or methansulfonic acid (20 mM) for cations. The concentration of PMS was determined using a modified ABTS method [34]. The consumption of PMS was spectrophotometrically monitored at 415 nm (ε = 34,000 $M^{-1}\,cm^{-1}$) using a UV/visible spectrophotometer (Agilent, 8453). The removal of total organic carbon (TOC) in amino acid solution was monitored using a TOC analyzer (Shimadzu TOC-V_{SH}).

For electron paramagnetic resonance (EPR) analysis, 5,5-dimethyl-1-pyrroline-N-oxide (DMPO) was used as a spin-trapping agent for SO4·$^-$ and ·OH. The EPR spectra of ROS adducts were monitored using a JES-TE 300 spectrometer (JEOL, Japan). The EPR measurement conditions were as follows: microwave power, 3 mW; microwave frequency, 9.42 GHz; center field, 338.25 mT; modulation width, 0.2 mT; and modulation frequency 100 kHz. The concentration of H_2O_2 was estimated using a colorimetric DPD method [35]. The generation of H_2O_2 was monitored at 551 nm (ε = 21,000 $M^{-1}\,cm^{-1}$) using a UV–vis spectrophotometer (Agilent, 8453).

2.4. Photoelectrochemical measurements

Photoelectochemical (PEC) measurements were carried out using a TiO_2/FTO electrode immersed in an aqueous solution of amino acid. The TiO_2/FTO electrode was prepared using a doctor blade method as described previously [36]. The paste of TiO_2 in a carbowax was spread on an FTO glass. Then, the coated electrode was calcined at 450 °C for 30 min under air to burn out the organic binder. Pt wire, Ag/AgCl, and TiO_2/FTO were utilized as a counter electrode, a reference electrode and a working electrode, respectively. The photoanode was immersed in $LiClO_4$ (for photocurrent measurement, 10 mM) or $NaClO_4$ (for EIS, 0.1 M) solution which contained 10 mM amino acid. The electrode was biased at +0.5 V (vs. Ag/AgCl) during photocurrent measurement and +1.0 V (vs. Ag/AgCl) during EIS measurement under continuous Ar gas purging.

2.5. Time-resolved diffuse reflectance (TDR) measurements

The TDR spectroscopic measurements were performed using a laser flash photolysis spectrometer (LKS 80, Applied Photophysics) coupled with an Nd-YAG laser (Brilliant B, Quantel). Before the TDR measurement, the powder sample was flushed with N_2 for 30 min in a quartz cuvette closed by a septum cap. The excitation wavelength was 355 nm for UV light (5 mJ/pulse) and 532 nm for visible light (70 mJ/pulse). In both cases, the laser pulse length was 5–6 ns and the irradiated area was 1 cm^2. The analyzing light from a 150 W xenon arc lamp was focused onto the sample surface and the reflected light was collected by a focusing lens (Spectrosil®) and directed through a monochromator to a detector (Hamamatsu photomultiplier R928). The detector was connected to an oscilloscope (DSO 9064A, Agilent) and subsequently to a computer interface. The collected absorption signal was converted to the reflectance signal (ΔJ) through the equation of $\Delta J = 1–10^{-Abs}$.

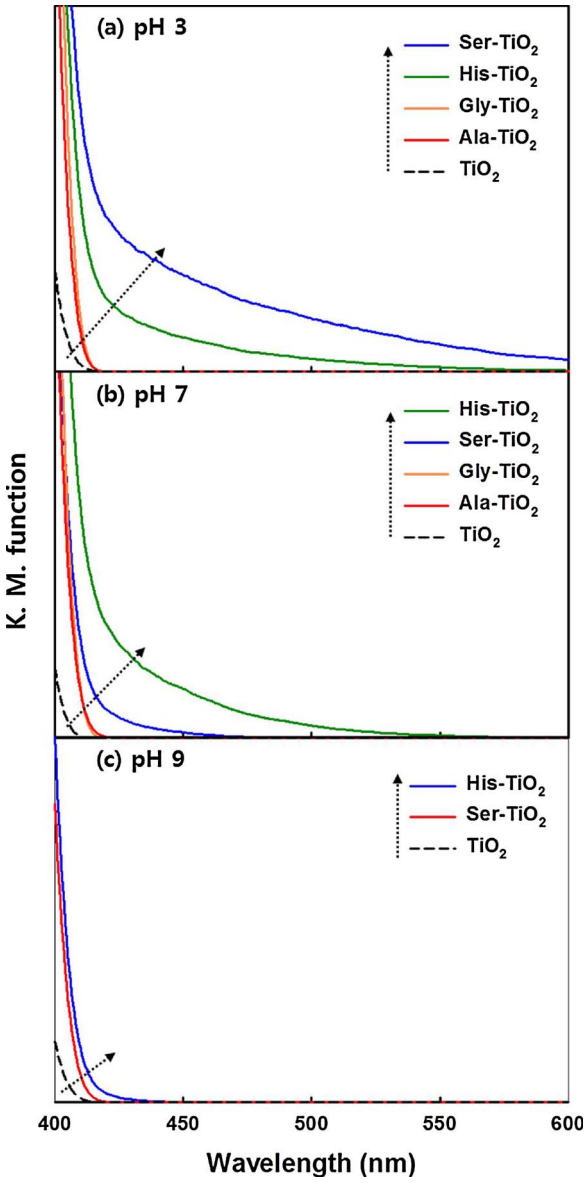

Fig. 1. Diffuse reflectance UV–visible spectra (DRS) of amino acid-TiO_2 complexes prepared at (a) pH 3, (b) pH 7, and (c) pH 9.

3. Results and discussions

3.1. Characterization of amino acid complexed-TiO_2

Fig. 1 shows the UV/visible diffuse reflectance spectra of various amino acid adsorbed-TiO_2 (AA/TiO_2) prepared at pH 3, 7, and 9. Bare TiO_2 exhibited negligible visible light absorption because of its wide bandgap (3.0–3.2 eV) [37]. When serine or histidine was adsorbed on the surface of TiO_2, the visible light absorption was significantly increased through LMCT mechanism [38]. The visible light absorption of Ser-TiO_2 was higher than that of His-TiO_2 at pH 3 (Fig. 1a), but the order of visible light absorption was reversed at pH 7 (Fig. 1b). The visible light absorption of serine- and histidine-TiO_2 was significantly reduced at pH 9 (Fig. 1c). This result should be ascribed to the different electrostatic interaction of amino acids with TiO_2 surface depending on pH (*see* Scheme S1). Since the molecular charge of serine and histidine is neutral and positive, respectively, at pH 3, serine experiences little repulsive force whereas histidine is electrostatically repelled by the positive surface charge of TiO_2 ($pH_{zpc} \approx 6$) [39] at pH 3. At pH 7, on the other hand, since the molecular charge of both serine and histidine

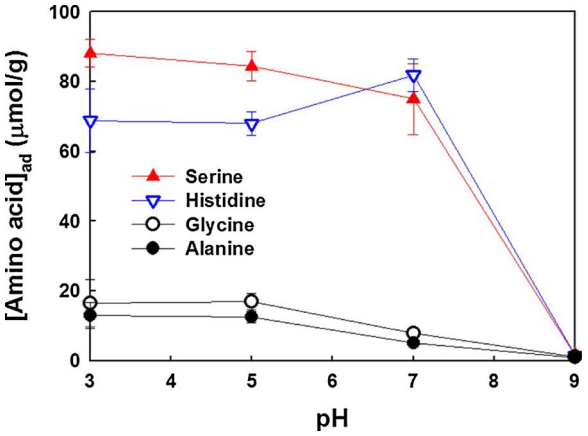

Fig. 2. pH-dependent adsorption of amino acids in aqueous suspension of TiO_2. The experimental conditions were [TiO_2] = 1 g/L, [amino acid] = 100 μM.

is neutral, they experience little electrostatic interaction with the charged TiO_2 surface. However, the imidazole ring and amine group in histidine interact with Ti atoms and O atoms via H-bonds on TiO_2 surface, respectively, which might promote the surface complexation of histidine on TiO_2 at pH 7 [40]. As a result, the AA/TiO_2 surface complexation, which is responsible for visible light absorption, is stronger with serine at pH 3 but weaker with serine at pH 7, compared with that of histidine. At pH 9, both amino acids and TiO_2 surface are negatively charged and consequently their surface complexation and the visible light absorption should be markedly hindered. On the other hand, the visible light absorption of alanine-TiO_2 and glycine-TiO_2 was negligible and not affected by pH. The amino acids which contain −OH (Ser) and −NH (His) in the side chain induce visible light absorption upon their complexation on TiO_2, whereas amino acids with $-CH_3$ (Ala) and no side chain (Gly) induce little visible light absorption. This implies that the surface adsorption of amino acids and their visible light absorption through LMCT complexation should be sensitively affected by the kind of the side chain and pH. Fig. 2 compares the pH-dependent adsorption of amino acids in aqueous suspension of TiO_2. Serine was more adsorbed on TiO_2 surface than histidine at acidic condition but the adsorption of histidine was slightly higher than that of serine at pH 7, above which the adsorption of both serine and histidine rapidly decreased with increasing pH. This pH-dependent trend agrees with that of DRS (*see* Fig. 1). In the case of glycine and alanine, their adsorption on TiO_2 was not significant over a wide pH range, which is also consistent with their low visible light absorption (Fig. 1). All the results support that the visible light absorption and the surface adsorption of amino acids on TiO_2 are strongly related and influenced by pH.

The complexation of amino acids on TiO_2 surface was investigated by FTIR spectroscopic measurements (Fig. S1). The characteristic IR bands in serine were confirmed at 1010, 1409, and 1572 cm^{-1}, which correspond to C−H rocking vibration of CH_2, C=O stretching vibration of COO^-, and N−H bending vibration of NH_3^+, respectively (Fig. S1a) [41]. In the case of histidine, similar peaks were confirmed and additional peaks were further observed at 1081 and 1627 cm^{-1}, which are ascribed to the C−N stretching band and C=C stretching band of imidazole ring, respectively (Fig. S1b) [42]. The surface-complexed amino acids on TiO_2 surface was further confirmed by performing electron energy loss spectroscopy (EELS) elemental mapping analysis (Fig. S2). The uniform distribution of Ti, C and N elements within the amino acid complexed-TiO_2 sample was confirmed (Fig. S2a–h), whereas bare TiO_2 exhibited the absence of C and N (Fig. S2i–l). All the analysis results of DRS, adsorption isotherm, FTIR, and EELS indicate the surface complexation of serine and histidine on TiO_2 is responsible for the visible light absorption.

3.2. pH effect on visible light activation of PMS

The strong surface complexation between amino acids (AA) and TiO_2 excites electrons via LMCT under visible light (Eq. (1)) and subsequently, the injected electron can be either recombined (Eq. (2)) or transferred to PMS to generate sulfate anion (Eq. (3)) [43] and sulfate radical (Eq. (4)) [44]. After the LMCT-induced electron transfer, AAs should be oxidatively degraded (Eq. (5)).

$$\text{AA-TiO}_2 + h\nu\ (\lambda > 420\ \text{nm}) \rightarrow (\text{AA}\cdot^+) - \text{TiO}_2\ (e_{cb}^-) \quad (1)$$

$$(\text{AA}\cdot^+) - \text{TiO}_2\ (e_{cb}^-) \rightarrow \text{AA-TiO}_2 \quad (2)$$

$$HSO_5^- + H^+ + 2e_{cb}^- \rightarrow SO_4^{2-} + H_2O \quad (3)$$

$$HSO_5^- + e_{cb}^- \rightarrow SO_4\cdot^- + OH^- \quad (4)$$

$$\text{AA}\cdot^+ + O_2 \rightarrow\rightarrow \text{degradation products (}e.g.,\ NH_4^+\text{)} \quad (5)$$

Since the LMCT sensitization requires the formation of surface complexes, PMS activation by visible light-induced LMCT between adsorbed AA and TiO_2 should be highly dependent on pH. Fig. 3a and b shows the time profiles of NH_4^+ production (from the degradation of serine and histidine) and the accompanying decomposition of PMS under visible light at pH 3–9. The visible light-induced production of NH_4^+ and the decomposition of PMS with the degradation of serine progressively decreased with increasing pH (*highest at pH 3 and negligible at pH 9*) in the presence of PMS and TiO_2 (Fig. 3a). On the other hand, those of histidine increased with increasing pH from 3 to 7 but was negligible at pH 9 (Fig. 3b). This result is consistent with the pH-dependent visible light absorption of AA/TiO_2 complexes (Fig. 1) and surface adsorption of AA on TiO_2 (Fig. 2). At pH 9, all amino acids are negatively charged and hence their surface complexation on TiO_2 is inhibited by the electrostatic repulsion. As a result, the PMS activation is also hindered at pH 9 (Fig. 3a and b). Due to the low visible light absorption and weak adsorption of glycine and alanine on TiO_2 (*see* Figs. 1 and 2), their visible light-induced degradation in the presence of PMS and TiO_2 was negligible (Fig. S3). The absence of either TiO_2 (PMS + AA + *hv*) or light (PMS + AA + TiO_2 (dark)) did not induce any degradation of AA at all (Fig. S4). It is also noted that AA can be slightly degraded on TiO_2 under visible light even in the absence of PMS since the LMCT excitation of AA on TiO_2 can be followed by the self-decomposition (Eq. (1) + Eq. (5)). However, the visible light-induced degradation of AA on TiO_2 is limited without PMS, which implies that the injected electrons undergo rapid back recombination (Eq. (2)). These control tests demonstrate that the decomposition of AA requires the simultaneous presence of TiO_2, PMS, and visible light. The activation of PMS (*i.e.*, its decomposition) is also enabled only when visible light, TiO_2, and AA are all co-present (*see* Fig. 3a & b). The direct visible light photolysis of PMS and AA is negligible and there is no dark catalytic activation of PMS on TiO_2 surface, either (*see* Fig. S5). Incidentally, PMS was slightly decomposed on TiO_2 even in the absence of AA under visible light (Fig. S5), which can be ascribed to the LMCT excitation of PMS itself on TiO_2.

The photocatalytic degradation of AAs on UV-illuminated TiO_2 generates NH_4^+, NO_3^-, and NO_2^- as products [8,45,46]. All of these products were also confirmed in this work from the degradation of serine (at pH 3) and histidine (at pH 7) on TiO_2 under UV light (Fig. 3c and d). The addition of PMS in the UV-irradiated TiO_2 suspension reduced but did not inhibit the generation of NO_3^- and NO_2^- completely (Fig. S6). The direct photolysis of AAs under UV light (in the absence of TiO_2 and PMS) was not observed at all (Fig. S7). On the other hand, only NH_4^+ was produced without showing any sign of NO_3^- and NO_2^-

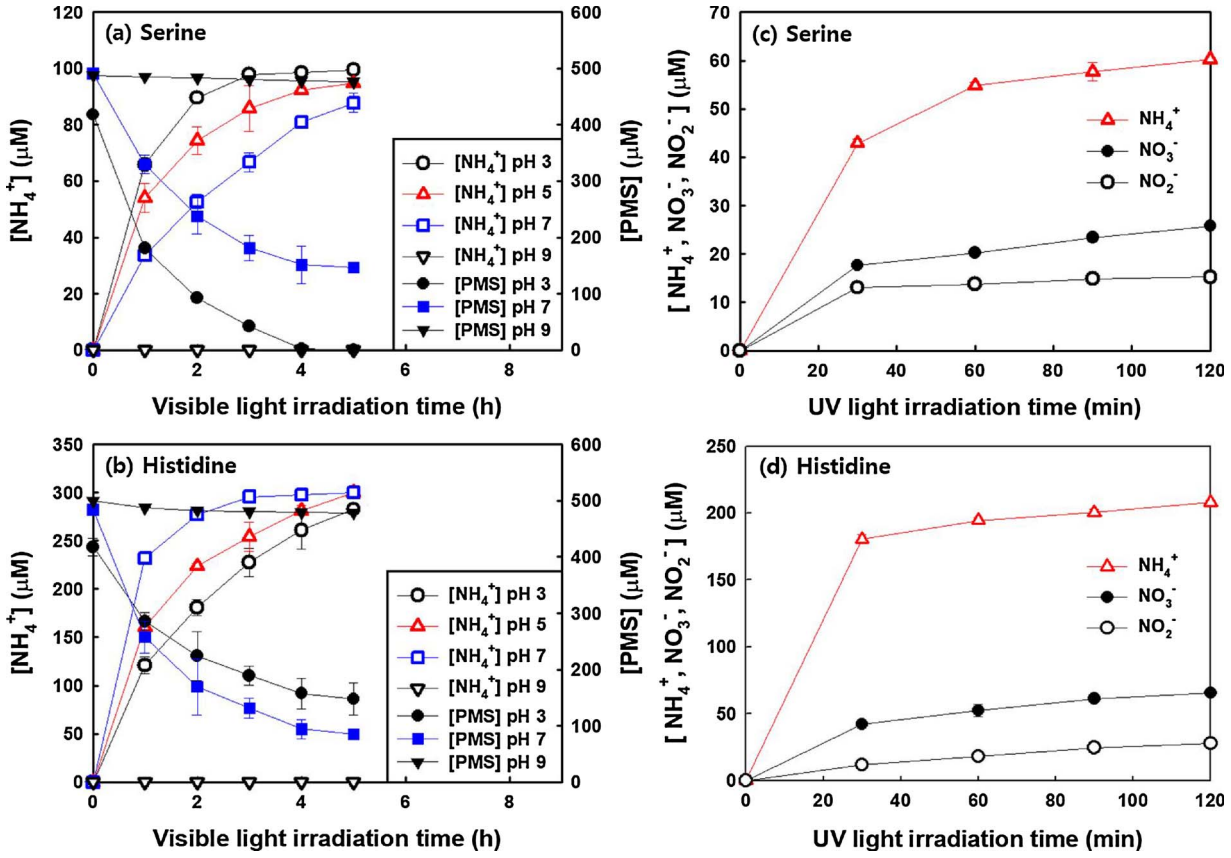

Fig. 3. (a, b) Time profiles of NH_4^+ production and PMS decomposition during the degradation of serine and histidine in PMS/TiO_2/visible light system at various pH. (c, d) Time profiles of NH_4^+, NO_2^-, and NO_3^- generation from the degradation of serine and histidine in TiO_2/UV system without PMS (pH = 3 for serine and 7 for histidine) for comparison with PMS/TiO_2/visible light system. The experimental conditions were [TiO_2] = 1 g/L, [PMS] = 500 μM (*for (a), (b)*), [amino acid] = 100 μM, λ > 420 nm (for visible light) or λ > 300 nm (for UV light), and air-equilibrated.

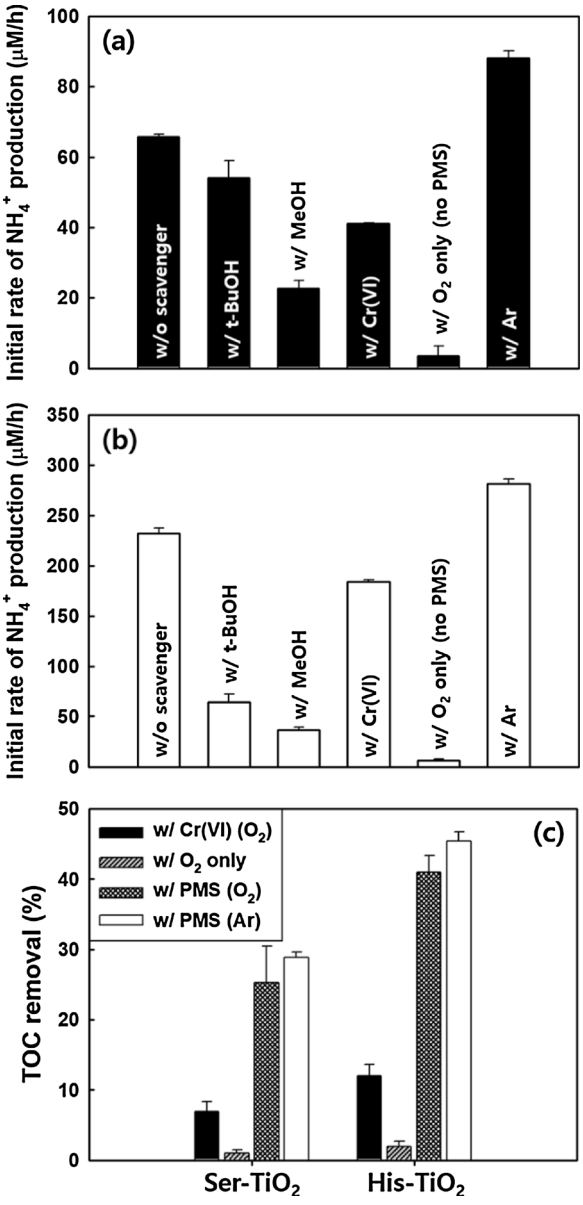

Fig. 4. Initial rate of NH_4^+ production from degradation of (a) serine at pH 3 and (b) histidine at pH 7 in the presence of methanol, t-BuOH, Cr(VI), and saturated Ar. The reference condition of "without scavenger" refers to the condition of AA/TiO_2/PMS/visible light in air-equilibrated suspension. The condition of "O_2 only (no PMS)" refers to AA/TiO_2/visible light under air-equilibration. (c) TOC removal after 5 h visible light irradiation. The experimental conditions were [TiO_2] = 1 g/L, [PMS] = 500 μM, [amino acid] = 100 μM, [MeOH] = [t-BuOH] = 100 mM, [Cr(VI)] = 10 mM, λ > 420 nm, air- or Ar-equilibrated.

generation under visible light (Fig. 3a and b). Serine has one nitrogen atom and histidine has three nitrogen atoms in the molecular structure and all the nitrogen atoms in AAs were quantitatively converted into NH_4^+ in the PMS/TiO_2/visible light system unlike the TiO_2/UV process. Therefore, the visible light-activated PMS on TiO_2 enables a selective and quantitative decomposition of AAs into NH_4^+.

3.3. Mechanism of PMS activation

For mechanistic investigation of PMS activation, the degradation of serine (at pH 3) and histidine (at pH 7) by PMS activated on TiO_2 was tested in the presence of various scavenger chemicals and control conditions: methanol (MeOH), *tert*-butanol (t-BuOH), and Cr(VI) as a preferential scavenger of $SO_4\cdot^-$, ·OH, and CB electron, respectively (Fig. 4). The reactions were also tested in a deaerated suspension (Ar saturation) to investigate the effect of dissolved O_2. The bimolecular rate constants for the reaction of ·OH with MeOH ($9.7 \times 10^8\,M^{-1}\,s^{-1}$) and t-BuOH ($6.0 \times 10^8\,M^{-1}\,s^{-1}$) are similar [10,47], but the rate constant for the reaction of $SO_4\cdot^-$ with MeOH ($3.2 \times 10^6\,M^{-1}\,s^{-1}$) is far higher than that with t-BuOH ($4.0 \times 10^5\,M^{-1}\,s^{-1}$) [10]. That is, while MeOH and t-BuOH scavenge ·OH with a similar efficiency, MeOH is a far more efficient scavenger of $SO_4\cdot^-$ than t-BuOH. Therefore, the difference in the inhibition effects between MeOH and t-BuOH can be ascribed to the role of MeOH as a scavenger of $SO_4\cdot^-$ [48]. The initial rate of NH_4^+ production from the degradation of serine was quenched by 17.8% with t-BuOH and 65.7% with MeOH (Fig. 4a), which indicates that serine is dominantly degraded by $SO_4\cdot^-$. However, the difference of inhibition effects between MeOH and t-BuOH was much smaller for histidine degradation at pH 7 (Fig. 4b). This might be ascribed to that $SO_4\cdot^-$ can be effectively converted into ·OH at alkaline pH through the following reaction.

$$SO_4\cdot^- + {}^-OH \rightarrow \cdot OH + SO_4^{2-}\ (6.5 \times 10^7\,M^{-1}\,s^{-1})\ [10] \quad (6)$$

Although the production rate of NH_4^+ from the degradation of serine and histidine was significantly reduced in the presence of radical scavengers (MeOH and t-BuOH), it was not completely quenched, implying that a non-radical pathway might also contribute to the degradation of serine and histidine. To test this, AA degradation was carried out in the presence of Cr(VI) as an alternative electron acceptor instead of PMS and in the absence of any electron acceptor (under Ar-purged condition without O_2) (Fig. 4). With Cr(VI) added instead of PMS (no $SO_4\cdot^-$ generation condition), the production of NH_4^+ from the degradation of serine and histidine was lower than that in the presence of PMS. However, the degradation of AAs was enabled even in the absence of PMS (with Cr(VI) as an electron acceptor), which indicates that the role of sulfate radical is not essential for the degradation of AA. This implies that AA can be oxidatively degraded upon injecting an electron into TiO_2 CB through LMCT mechanism (non-radical pathway). Either PMS or Cr(VI) serves as an electron acceptor upon the visible light-induced electron transfer from AAs to TiO_2. The LMCT-initiated oxidation of AA (Eq. (1) + Eq. (5)) leads to the degradation of AAs with the accompanied production of NH_4^+, which can proceed through a non-radical mechanism. However, this non-radical degradation mechanism does not seem to be effective in mineralization since the TOC removal efficiency was low when Cr(VI) was present as an alternative electron acceptor instead of PMS (*see* Fig. 4c). In the O_2 only (no PMS) condition, the degradation of AA was negligibly low. The generation of $SO_4\cdot^-$ is critical for the efficient degradation/mineralization of AAs and this radical generation should be initiated by the electron transfer (Eq. (4)). On the other hand, the role of dissolved O_2 in the AA/TiO_2/PMS/visible light system was also investigated. It should be noted that both PMS and O_2 are competing electron acceptors and O_2 is generally needed for the mineralization of organic compounds. When dissolved O_2 was removed by Ar purging, both degradation and mineralization of AAs in the suspension of PMS and TiO_2 under visible light was enhanced (Fig. 4). This should be ascribed to the fact that the absence of competing electron acceptors (O_2) enables more electrons to be transferred to PMS with generating more $SO_4\cdot^-$. The fact that the mineralization of AAs was even enhanced in the absence of O_2 (Ar-saturated) implies that PMS should supply the oxygen needed for the mineralization of AAs. AAs can be degraded by both LMCT (non-radical pathway, Scheme 1a) and $SO_4\cdot^-$ (radical pathway, Scheme 1b) mediated mechanisms.

We confirmed radical species generated in PMS/TiO_2/AAs under visible light using EPR spin-trapping technique (Fig. 5). The visible light irradiation immediately generated radical signals. It is interesting to note that DMPO-OH and DMPO-SO_4 signals were detected even with bare TiO_2 under visible light, which indicates that some PMS can be directly activated on visible light-irradiated TiO_2 without the need of

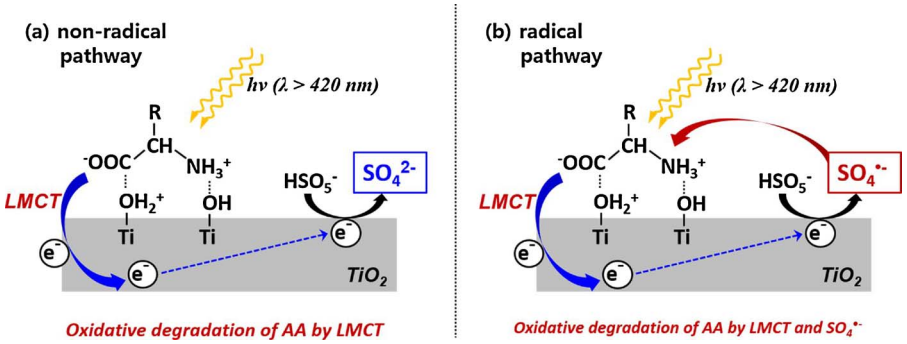

Scheme 1. Schematic illustration of (a) non-radical and (b) radical pathway for the degradation of amino acids by activating PMS under visible light.

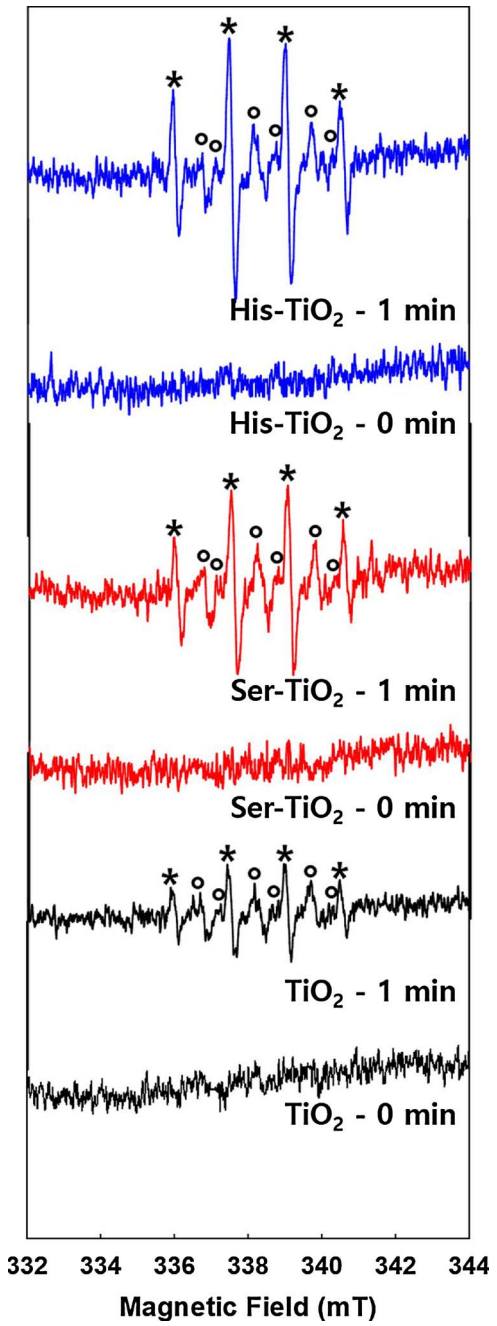

Fig. 5. EPR spectra of OH-DMPO (*) and SO_4-DMPO (°) generated on bare TiO_2, Ser-TiO_2, and His-TiO_2 under visible light. The experimental conditions were [TiO_2] = 1.5 g/L, [PMS] = 2 mM, [amino acid] = 1 mM, [DMPO] = 90 mM, pH = 3 (for bare- and Ser-TiO_2) or 7 (for His-TiO_2), λ > 420 nm, air-equilibrated.

AA. This phenomenon is consistent with the observation that some PMS could be degraded on bare TiO_2 under visible light (*see* Fig. S5) and supports that PMS complexed on TiO_2 can be directly activated under visible light as AA complexed on TiO_2 is excited through LMCT mechanism. However, the radical signal intensity was significantly enhanced in the presence of serine (at pH 3) and histidine (at pH 7) on TiO_2 surface. This further indicates that $SO_4\cdot^-$ from PMS can be generated mainly through the LMCT excitation of AA/TiO_2 (Eqs. (1)–(4)). The accompanying production of ·OH can be ascribed to the conversion of sulfate radical through Eq. (6) or the reductive transformation of O_2 through sequential electron transfers ($O_2 \rightarrow H_2O_2 \rightarrow$ ·OH). To investigate which pathway is contributing to the production of ·OH, the visible light-induced production of H_2O_2 in the aqueous suspension of histidine/TiO_2 was compared in the presence and absence of PMS (*see* Fig. S8). The production of H_2O_2 was significantly inhibited in the presence of PMS, which implies that PMS effectively scavenges CB electrons with minimizing the electron transfer to O_2 in the histidine/TiO_2/visible light system. This result also implies that the observed production of ·OH in the AA/TiO_2/PMS under visible light should come mainly from the transformation of sulfate radical (Eq. (6)), not from the decomposition of H_2O_2. In a separate control test of ESR, UV/TiO_2 system generated the DMPO−OH signal only, not the DMPO-SO_4 signal at all (*see* Fig. S9).

3.4. Photoelectrochemical properties of amino acid complexed-TiO_2

The photoelectrochemical (PEC) behaviors of AA-adsorbed TiO_2 electrodes were compared at pH 3 and 7. The photocurrent generation (Fig. 6a and b) and the electrochemical impedance spectroscopy (EIS) Nyquist plot (Fig. 6c and d) were compared between serine-TiO_2 and histidine-TiO_2 under visible light. The photocurrent and the size of arc in the EIS Nyquist plot reflect the efficiency of LMCT sensitization and the resistance of charge transfer on the electrode surface under visible light, respectively. The higher photocurrent indicates that more charge carriers are generated and the smaller arc size in an EIS Nyquist plot reflects lower charge transfer resistance on the electrode [49]. Bare TiO_2 electrode exhibited the lowest photocurrent generation and the biggest arc size in the EIS Nyquist plot under visible light because of its inability to absorb visible light. The photocurrent generation was higher and the arc size was smaller with Ser-TiO_2 electrode than His-TiO_2 electrode at pH 3 under visible light, which indicates that more charge carriers are generated and the charge transfer is more efficient in Ser-TiO_2 than His-TiO_2. This trend was reversed at pH 7, which is consistent with the pH-dependent visible light absorption of AA/TiO_2 (Fig. 1), AA adsorption on TiO_2 (Fig. 2), and visible light activation of PMS (Fig. 3). The fact that the pH-dependent PEC behaviors of AA/TiO_2 electrodes (Fig. 6) agree with other pH-dependent behaviors of AA/TiO_2 (Figs. 1–3) implies that the surface complexation of AAs on TiO_2 and its LMCT excitation are responsible for the visible light activation of PMS.

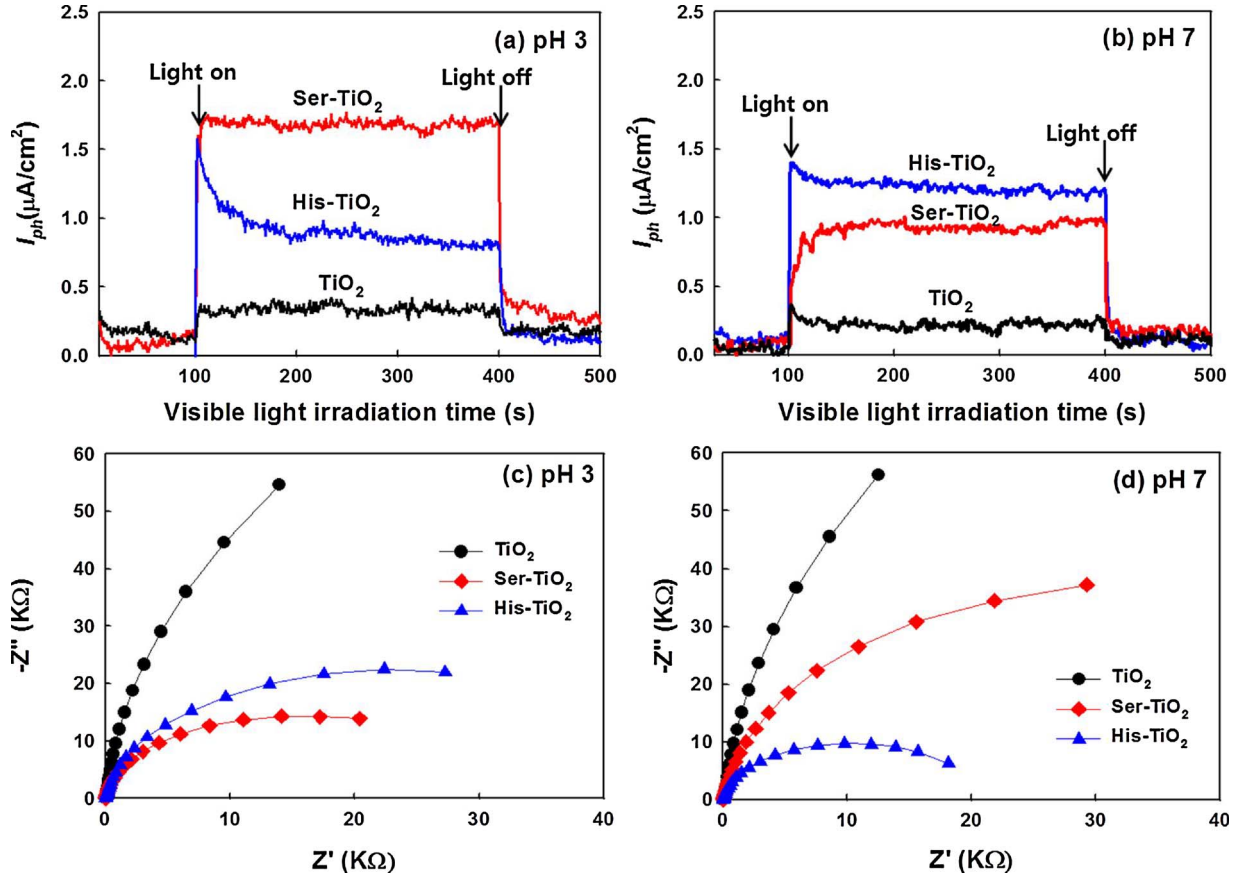

Fig. 6. Time profiles of photocurrent generation with amino acid-TiO_2/FTO electrode under visible light irradiation at (a) pH 3 and (b) pH 7. Electrochemical impedance spectroscopic (EIS) Nyquist plots under visible light irradiation at (c) pH 3 and (d) pH 7. The experimental conditions were [$NaClO_4$] = 10 mM, potential bias of +0.5 V (for photocurrent), 0 V (for EIS) (vs. Ag/AgCl). The electrolyte solution was continuously Ar-purged.

3.5. Charge carrier dynamics in amino acid-complexed TiO_2

To investigate the behaviors of charge carrier generated on AA/TiO_2, the photogenerated charge carriers were probed by time-resolved diffuse reflectance spectroscopy (Fig. 7). The AA/TiO_2 samples were compared with bare TiO_2. Laser excitation wavelength of 355 nm (for UV light) and 532 nm (for visible light) were employed. Prior to the experiment, all samples were flushed with N_2 for 30 min and sealed in gas-tight cells. The powder samples were measured under N_2 atmosphere to maximize the lifetime of the photogenerated electrons by preventing the electron transfer to adsorbed O_2.

After UV light excitation (355 nm), the transient absorption spectra of bare TiO_2 were recorded between 400 and 700 nm. The absorption in lower wavelengths (400–550 nm) is attributed to the trapped holes and that in the higher wavelengths (600–800 nm) is ascribed to the trapped electrons (Fig. 7a) [50,51]. In the presence of histidine and serine on the TiO_2 surface, the absorption signal intensities at shorter wavelengths decreased, whereas those at longer wavelengths increased in comparison to bare TiO_2 (Fig. 7b and c). This result indicates that AA/TiO_2 under UV irradiation reduced the concentration of trapped holes but increased the trapped electron concentration. This is expected because the adsorbed AAs should serve as a hole scavenger with retarding the charge pair recombination and increasing the lifetime of the photogenerated electrons in TiO_2. The transient absorption of bare TiO_2 decayed much slowly at 400 nm (trapped hole) but faster at 640 nm (trapped electron) than that of AA complexed-TiO_2 (Fig. S10a and b), which further supports that AAs act as a hole scavenger under UV light and subsequently increases the electron lifetime. On the other hand, in the case of visible light excitation (532 nm), no transient absorption signals of electrons and holes could be detected for bare TiO_2 (Fig. 7d), which was expected since the large bandgap TiO_2 cannot be excited by visible light irradiation. Nevertheless, transient absorption signals at 600–700 nm appeared in the presence of AAs on TiO_2 (Fig. 7e and f), which implies that the trapped electrons are generated upon visible light irradiation. The LMCT between AA and TiO_2 should be responsible for the transient absorption signal induced by visible light. This is also consistent with the absence of the trapped hole signal under visible light because LMCT cannot excite VB holes. The trapped electron signal caused by LMCT has a much shorter lifetime (< 25 ns) compared with the UV-excited electron (Fig. S11). All the transient spectral data support that AA adsorbed on TiO_2 generated electrons only (not holes) under visible light via LMCT mechanism and this should be responsible for the activation of PMS.

4. Conclusions

This study demonstrated that amino acids (common aquatic pollutants) can activate PMS under visible light through forming heterogeneous surface complexes on titania catalyst. Although there have been a variety of approaches in activating PMS, the present method is unique in that the contaminant itself serves as an activator of PMS. Utilization of visible light is another merit which distinguishes this method from other photochemical activation methods using UV light. In particular, NH_4^+ was generated as a sole nitrogenous product from the degradation of amino acids, whereas other oxidation processes of amino acids (*e.g.*, chlorination [5], TiO_2/UV [8]) generate various toxic products such as disinfection byproducts (DBPs), NO_3^- and NO_2^-. This PMS activation method is environmentally favored because of the use of nontoxic and durable material (TiO_2 catalyst) and mild energy input (visible light).

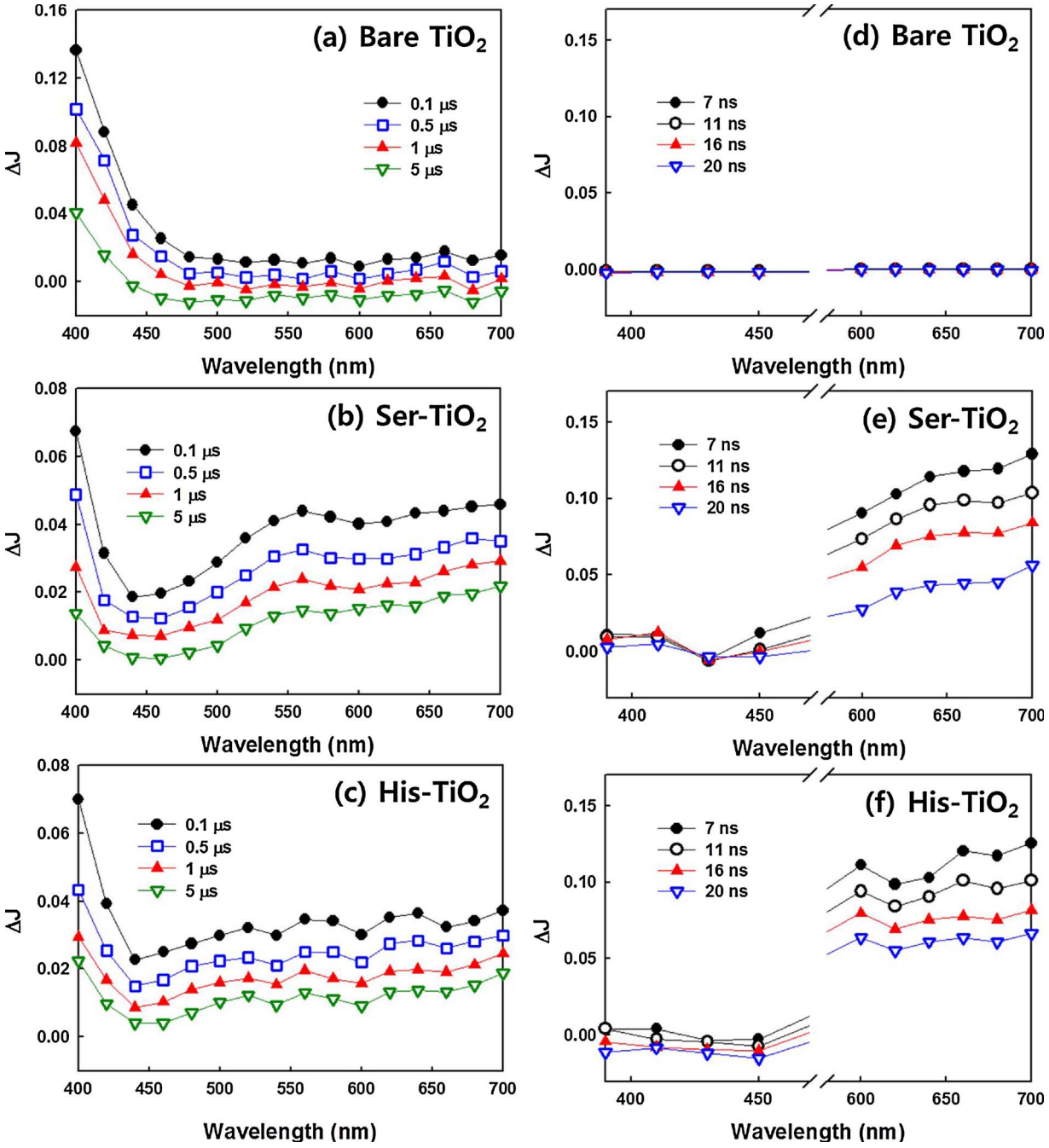

Fig. 7. Transient absorption spectra of TiO_2, Ser-TiO_2, and His-TiO_2 measured (a-c) at 0.1, 0.5, 1, and 5 μs after laser excitation (λ_{ex} = 355 nm for UV light) and (d-f) at 7, 11, 16, and 20 ns after laser excitation (λ_{ex} = 532 nm for visible light) under N_2 atmosphere.

Acknowledgements

This work was supported by Global Research Laboratory (GRL) Program (NRF-2014K1A1A2041044) and Basic Science Research Program (NRF-2017R1A2B2008952), which were funded by the Korea government (MSIP) through National Research Foundation of Korea (NRF). We appreciate the late Dr. Alok Bokare for his valuable discussion and comments.

Appendix A. Supplementary data

Supplementary data associated with this article can be found, in the online version, at https://doi.org/10.1016/j.apcatb.2017.12.025.

References

[1] H. Lachheb, D.A. Houas, C. Guillard, J. Photochem. Photobiol. A: Chem. 246 (2012) 1.
[2] S. Fernando, C. Hall, S. Jha, Energy Fuels 20 (2006) 376.
[3] J.M. Holloway, R.A. Dahlgren, B. Hansen, W.H. Casey, Nature 395 (1998) 785.
[4] E. Pehlivanoglu, D.L. Sedlak, Water Res. 38 (2004) 3189.
[5] S. Weng, E.R. Blatchley, Environ. Sci. Technol. 47 (2013) 4269.
[6] C. Na, T.M. Olson, Environ. Sci. Technol. 40 (2006) 1469.
[7] E. Szabó-Bárdos, K. Somogyi, N. Törő, G. Kiss, A. Horváth, Appl. Catal. B: Environ. 101 (2011) 471.
[8] H. Hidaka, S. Horikoshi, K. Ajisaka, J. Zhao, N. Serpone, J. Photochem. Photobiol. A: Chem. 108 (1997) 197.
[9] Y. Zhou, J. Jiang, Y. Gao, J. Ma, S.-Y. Pang, H. Li, X.-T. Lu, L.-P. Yuan, Environ. Sci. Technol. 49 (2015) 12941.
[10] Y.-H. Guan, J. Ma, X.-C. Li, J.-Y. Fang, L.-Y. Chen, Environ. Sci. Technol. 45 (2015) 9308.
[11] M. Spiro, Electrochim. Acta 24 (1979) 313.

[12] R.E. Huie, C.L. Clifton, P. Neta, Radiat. Phys. Chem. 38 (1991) 477.
[13] J. Sun, X. Li, J. Feng, X. Tian, Water Res. 43 (2009) 4363.
[14] Y. Feng, D. Wu, Y. Deng, T. Zhang, K. Shih, Environ. Sci. Technol. 50 (2016) 3119.
[15] T. Zhang, H. Zhu, J.-P. Croué, Environ. Sci. Technol. 47 (2013) 2784.
[16] Y.-Y. Ahn, E.-T. Yun, J.-W. Seo, C. Lee, S.H. Kim, J.-H. Kim, J. Lee, Environ. Sci. Technol. 50 (2016) 10187.
[17] G.P. Anipsitakis, D.D. Dionysiou, Environ. Sci. Technol. 38 (2004) 3705.
[18] X. Duan, Z. Ao, H. Sun, L. Zhou, G. Wang, S. Wang, Chem. Commun. 51 (2015) 15249.
[19] X. Wang, Y. Qin, L. Zhu, H. Tang, Environ. Sci. Technol. 49 (2015) 6855.
[20] X. Duan, H. Sun, J. Kang, Y. Wang, S. Indrawirawan, S. Wang, ACS Catal. 5 (2015) 4629.
[21] G.P. Anipsitakis, D.D. Dionysiou, Appl. Catal. B: Environ. 54 (2004) 155.
[22] F. Ghanbari, M. Moradi, J. Chem. Eng. 310 (2017) 41.
[23] K. Zhu, J. Wang, Y. Wang, C. Jin, A.S. Ganeshraja, Catal. Sci. Technol. 6 (2016) 2296.
[24] Y. Liu, H. Guo, Y. Zhang, W. Tang, X. Cheng, H. Liu, Chem. Phys. Lett. 653 (2016) 101.
[25] G. Zhang, G. Kim, W. Choi, Energy Environ. Sci. 7 (2014) 954.
[26] J. Lim, D. Monllor-Satoca, J.S. Jang, S. Lee, W. Choi, Appl. Catal. B: Environ. 152–153 (2014) 233.
[27] S. Kim, W. Choi, J. Phys. Chem. B 109 (2005) 5143.
[28] G. Zhang, W. Choi, Chem. Commun 48 (2012) 10621.
[29] Y. Park, N.J. Singh, K.S. Kim, T. Tachikawa, T. Majima, W. Choi, Chem. Eur. J. 15 (2009) 10843.
[30] Y. Wang, K. Hang, N.A. Anderson, T. Lian, J. Phys. Chem. B 107 (2003) 9434.
[31] S. Kaniyankandy, S. Rawalekar, A. Sen, B. Ganguly, H.N. Ghosh, J. Phys. Chem. C 116 (2012) 98.
[32] G. Kim, W. Choi, Appl. Catal. B: Environ. 100 (2010) 77.
[33] G. Kim, S.-H. Lee, W. Choi, Appl. Catal. B: Environ. 162 (2015) 463.
[34] Y. Yang, J. Jiang, X. Lu, J. Ma, Y. Liu, Environ. Sci. Technol. 49 (2015) 7330.
[35] H. Bader, V. Sturzenegger, J. Hoigné, Water Res. 22 (1988) 1109.
[36] Y. Park, S.-H. Kang, W. Choi, Phys. Chem. Chem. Phys. 13 (2011) 9425.
[37] J. Lim, P. Murugan, N. Lakshiminarasimhan, J.Y. Kim, J.S. Lee, S.-H. Lee, W. Choi, J. Catal. 310 (2014) 91.
[38] S. Kim, G.-h. Moon, G. Kim, U. Kang, H. Park, W. Choi, J. Catal. 346 (2017) 92.
[39] J. Kim, C.W. Lee, W. Choi, Environ. Sci. Technol 44 (2010) 6849.
[40] I.A. Mudunkotuwa, V.H. Grassian, Langmuir 30 (2014) 8751.
[41] K. Rajesh, P.P. Kumar, J. Mater. 2014 (2014) 1.
[42] T. Noguchi, T. Inoue, X.-S. Tang, Biochemical 38 (1999) 10187.
[43] M. Spiro, Electrochim. Acta 24 (1979) 313.
[44] H. Lee, H.-i. Kim, S. Weon, W. Choi, Y.S. Hwang, J. Seo, C. Lee, J.-H. Kim, Environ. Sci. Technol. 50 (2016) 10134.
[45] S. Horikoshi, H. Hidaka, N. Serpone, J. Photochem. Photobiol. A: Chem. 138 (2001) 69.
[46] X. Wang, S. Kim, C. Buda, M. Neurock, O.B. Koper, J.T. Yates, J. Phys. Chem. C 113 (2009) 2228.
[47] P. Neta, R.E. Huie, A.B. Ross, J. Phys. Chem. Ref. Data 117 (1988) 1027.
[48] G.V. Buxton, C.L. Greenstock, W.P. Helman, A.B. Ross, Phys. Chem. Ref. Data 17 (1988) 513.
[49] E.-H. Kong, J. Lim, H. Lee, W. Choi, H.M. Jang, Appl. Catal. B: Environ. 176 (2015) 76.
[50] J. Schneider, M. Matsuoka, M. Takeuchi, J. Zhang, Y. Horiuchi, M. Anpo, D.W. Bahnemann, Chem. Rev. 114 (2014) 9919.
[51] J. Schneider, K. Nikitin, M. Wark, D.W. Bahnemann, R. Marschall, Phys. Chem. Chem. Phys. 18 (2016) 10719.